

Tu SRS3 05

## Structurally Conformal Resolution Enhancement with Joint Sparse Inversion

C. Peng\* (CGG), B. Bai (CGG), Y. Liu (CGG) & Z. Fu (CGG)

### SUMMARY

---

Removing source wavelet and residual non-uniform absorption ( $Q$ ) effects can enhance the spatial resolution of seismic images after de-ghosting and amplitude attenuation compensation. In this abstract we propose a new resolution enhancement method that incorporates structural conformity constraints and sparse regularization into an inversion-based deconvolution. The method was applied to field data and compared with an inversion-based approach without sparse regularization and structural conformity constraints. The new method provides a resolution-enhanced broader bandwidth image with improved signal-to-noise ratio and geological coherence. Acoustic impedance inversion was carried out after resolution enhancement, and a more detailed and coherent impedance volume was obtained.

## Introduction

Seismic images with broad bandwidth are in demand for high resolution imaging of subsurface structures that may lead to more accurate interpretation. However, in reality bandwidth shrinkage of acquired seismic data is present for many reasons: non-uniform attenuation of the medium, free-surface ghost waves, and the bandwidth limitation of the seismic source itself. Many broadband technologies have been developed to address these issues. To remove the free-surface ghost, deghosting technologies have been proposed (Wang and Peng, 2012; Caprioli *et al.*, 2012). Although deghosting can reverse ghost-induced bandwidth shrinkage it leaves frequency attenuation effects, resulting in slanted spectra with a peak frequency shifted towards the low end. To compensate for frequency-dependent attenuation, various amplitude Q compensation methods have been proposed; however, they struggle with a loss in high frequency due to the stabilization requirements of the regularization and the difficulty in obtaining accurate Q models. Moreover, in principle, both deghosting and amplitude Q compensation cannot deal with bandwidth limitation due to the seismic source.

One approach to further enhance resolution is to remove residual source signature and non-stationary Q effects by deconvolution. Deconvolution methods can be classified into two main categories. The first is filtering-based deconvolution, in which a Wiener filter is calculated based on white spectrum reflectivity and minimum phase wavelet assumptions, or minimum entropy of reflectivity assumption, and applied to the seismic traces, e.g. (Berkhout 1977, Wiggins 1977, Yang and Soubaras 2015). However, these methods are very sensitive to parameters in the inverse filter estimation and can amplify noise. The second category is inversion-based deconvolution, in which a seismic wavelet is estimated first and the linear convolving equations are solved as a second inversion problem. Due to the limited bandwidth of the wavelet, deconvolution is an ill-posed problem and regularization is required to overcome the non-uniqueness of the solution. Compared with traditional  $L^2$  regularization that constrains the total energy of the deconvolved trace, sparse regularization gives a simpler and less noisy model that can explain the observations (Sacchi 1997). Performing deconvolution trace-by-trace may introduce inconsistencies and structural non-conformity among neighbouring traces, especially when sparse regularization is used. In this paper, we propose a sparse regularization-based joint inversion scheme that utilizes neighbouring traces to achieve a 3D structurally conformal and stable resolution enhancement (*RE*) by deconvolution.

## Method

Bandwidth shrinkage is usually modelled as:

$$d(t) = w(t) * r(t), \quad (1)$$

where  $d(t)$  is the seismic trace with limited bandwidth,  $w(t)$  is the bandwidth shrinkage operator (i.e. encoding residual source signature and absorption) and  $r(t)$  is the spiky reflectivity series. In deconvolution processing, the goal is to obtain a spectrum-broadened trace,  $r'(t)$ , which is closer to the real reflectivity series than  $d(t)$  is. The seismic wavelet can be estimated using autocorrelations combined with maximum kurtosis phase, multichannel estimation, or well log information. We do not address methods for estimation of wavelets here, but rather assume the local wavelets that incorporate residual Q effects has been estimated by one of these methods.

Traditional methods to recover the reflectivity from equation (1) are usually performed trace-by-trace. In this paper we propose to use an inversion with a reweighted sparse regularization. In addition, instead of solving the inversion trace-by-trace, we perform joint inversion for the central trace along with its neighbouring traces to better account for coherency along geological structures. In seismic stacks, the neighbouring traces may be considered as warped versions of each other, the linear warping operators being functions of the local geology. We therefore expand equation (1) as:

$$\begin{pmatrix} d_1 \\ \vdots \\ d_n \end{pmatrix} = \begin{pmatrix} \mathbb{P}_1 \\ \vdots \\ \mathbb{P}_n \end{pmatrix} \mathbb{W}r, \quad (2)$$

where  $d_i$  are neighbouring traces and  $d_{n/2}$  is the central trace, and  $\mathbb{P}_i$  are the warping operators that convert the central trace to its neighbor  $i$ . Thus,  $\mathbb{P}_{n/2} = \mathbb{I}$ .  $\mathbb{W}$  is a matrix to convolve the given wavelet.

The sharpened version of the central trace,  $r$ , is jointly inverted from equation (2) under a reweighted sparse regularization. The reweighting scheme (Trad, *et al.*, 2003) works by iteratively solving equation (3) by  $L^2$  regularization with the updated diagonal matrix,  $\mathbb{E}$ , in each iteration:

$$\begin{pmatrix} d_1 \\ \vdots \\ d_n \end{pmatrix} = \begin{pmatrix} \mathbb{P}_1 \\ \vdots \\ \mathbb{P}_n \end{pmatrix} \mathbb{W} \mathbb{E} x, \quad r = \mathbb{E} x. \quad (3)$$

Initially  $\mathbb{E}$  is set to the identity matrix, then in the next iteration the diagonal elements of  $\mathbb{E}$  are set to the envelope of  $r$  from the preceding iteration. Primary events are honoured and unnecessary ringing and noise energy are reduced in each iteration. Data-domain similarity weighting between the central trace and its neighbouring traces can be introduced into equation (3) to avoid smearing across faults. Due to the sparse regularization and structurally conformal constraints introduced by the neighbouring traces, clean and geologically conformal and resolution enhanced results are obtained.

## Examples

The first example is a pre-stack depth migrated stack from offshore West Africa. These data were acquired in a narrow azimuth (NAZ), variable-depth streamer configuration and had both receiver and source side deghosting applied. Although the ghost notches were removed and the bandwidth was extended accordingly, the spectrum was slanted with a peak frequency shifted towards the low end. Figure 1a is a zoom-in section of the stack that contains much faulting. Figure 1b shows the *RE* result with conventional  $L^2$  regularization without any structural conformity constraint. Although essentially the events became sharper and the spectrum became broader as shown by the black line in Figure 1d, considerable noise was amplified and some events became broken up. By comparison, Figure 1c shows the result with the new *RE* method; the image is cleaner, and the sharpened events are more coherent along the geological structures. The spectrum indicates that more high frequency energy was recovered by the new method.

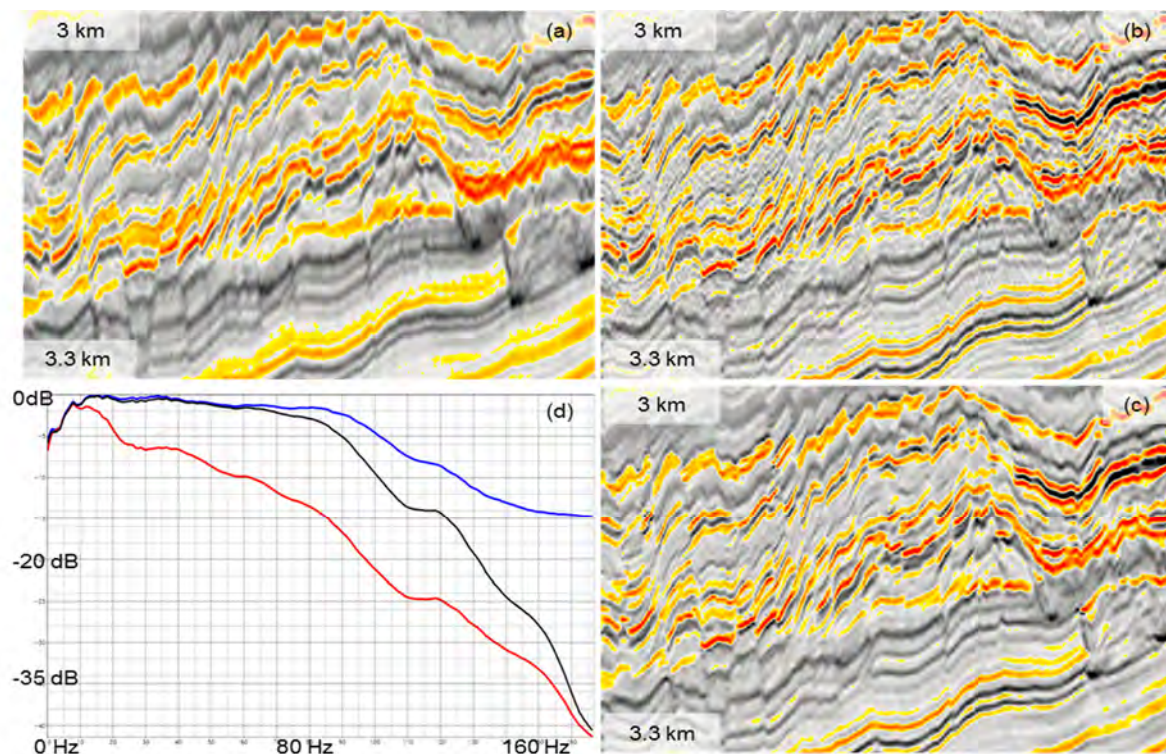


**Figure 1** (a) Input stack; (b) *RE* result without sparseness and structural conformity constraints; (c) structurally conformal *RE* based on joint sparse inversion; (d) Spectra of (a)(red line), (b)(black line), and (c)(blue line).

Figure 2 shows an inline section of the data before (Figure 2a) and after (Figure 2b) *RE* with the proposed method. Figures 2c and 2d show the spectrum became both broader and flatter at different depths. The structures in the depth slice appear more focused, and more structural details were revealed after the 3D structurally conformal *RE*, as shown in Figures 2e and 2f.

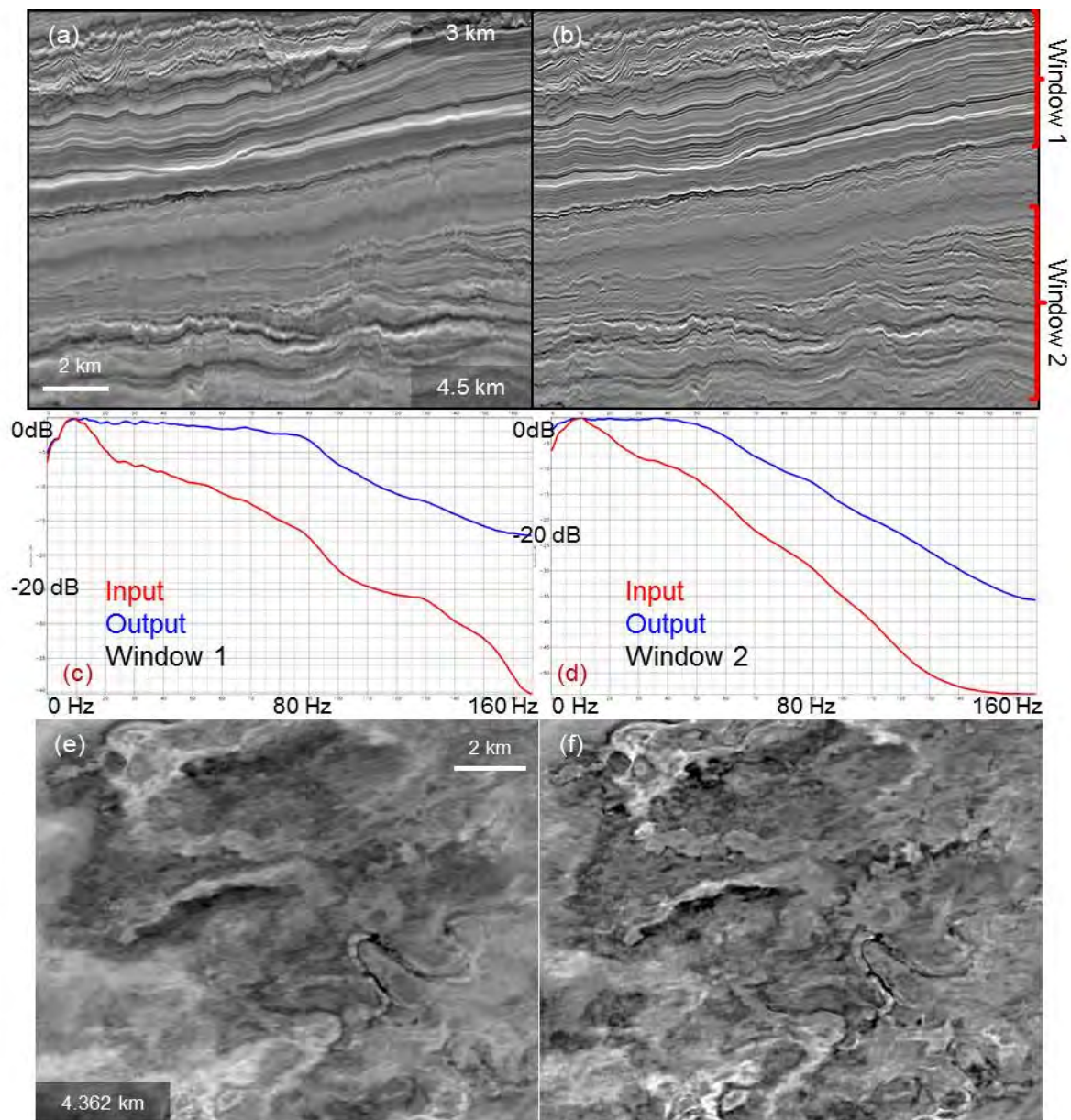


**Figure 2** (a) Stack before *RE*; (b) stack after *RE* with current method; (c) spectra of stack before and after *RE* in Window 1; (d) Spectra of stack before and after *RE* in Window 2; (e) depth slice at 4.362 km before *RE*; (f) same depth slice after *RE*.

Improving quantitative interpretation is the end goal of broadening the seismic spectrum and enhancing resolution. In the second data set, we demonstrate the impact of our method on impedance inversion of the seismic stack. Figure 3a shows the depth-migrated stack, stretched to time, from the East Breaks area of the Gulf of Mexico; the data were acquired using a flat-tow NAZ acquisition. Figure 3b shows the corresponding inverted impedance map. Figure 3c shows the more coherent and broadband seismic after the 3D structurally conformal *RE*; a more coherent and detailed impedance map was obtained based on the resolution enhanced seismic as shown in Figure 3d. Examining the target region around 3.5 sec, we see that the inverted impedance better matches the impedance well log after *RE* with the structurally conformal method.

## Conclusions

We have proposed a new resolution enhancement method that incorporates joint sparse inversion and a 3D structure conformity constraint. Due to the sparsity regularization, the method achieves good discrimination against noise energy; high frequency signals are boosted while the noise energy in the same band is suppressed. The 3D structural conformity constraint helps preserve the conformity of the resolution enhanced output with the geological structures. After *RE* with this method, we observe the seismic to have not only broader bandwidth and higher resolution, but also a higher signal-to-noise ratio and improved coherence along events. The enhanced resolution and improved coherence may lead to better seismic inversion of acoustic impedance with finer spatial resolution and higher geological coherence.

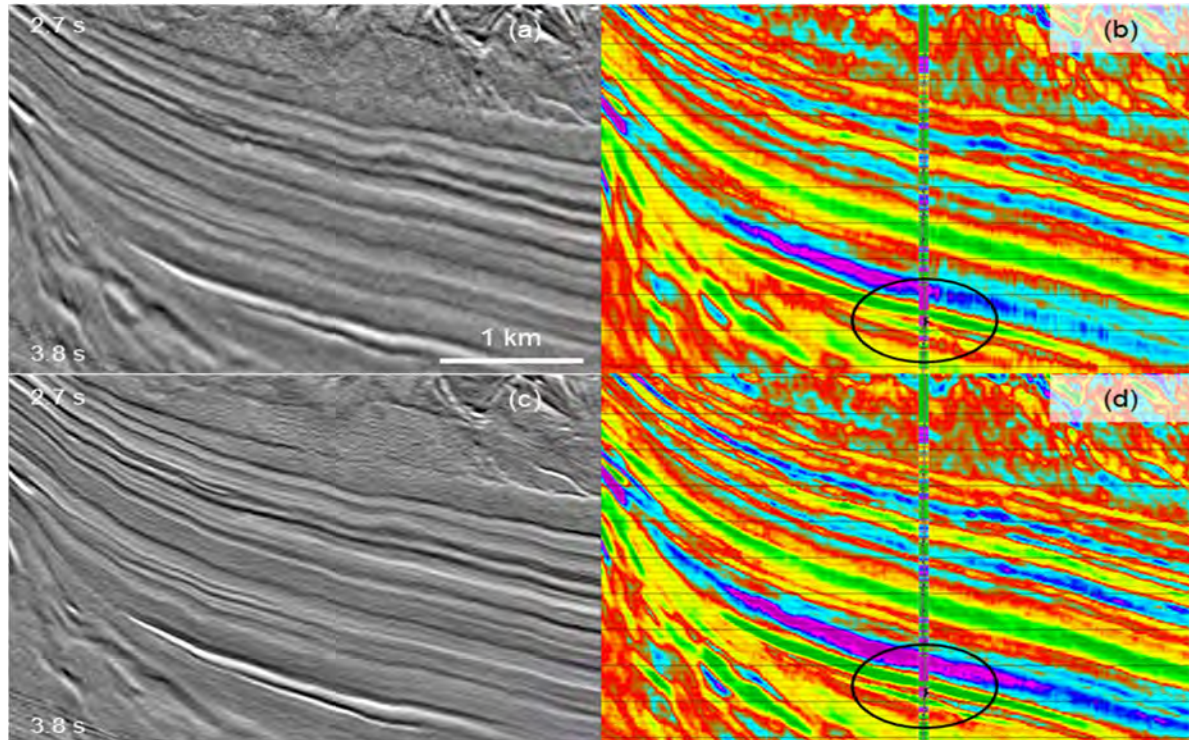


**Figure 3** (a) input seismic near target region; (b) impedance map inverted from input seismic; (c) seismic after *RE* with new method; (d) impedance map inverted from seismic after *RE* with new method.

## Acknowledgements

We thank CGG for permission to publish this work.

## References

- Berkhout, A.J. [1977] Least-Squares Inverse Filtering and Wavelet Deconvolution. *Geophysics*, **42**, 1369-1383
- Caprioli, P.B.A., Özdemir, A.K., Özbek, A., Kragh, J.E., van Manen, D.J., Christi, P.A.F. and Robertsson, J.O.A. [2012] Combination of Multi-component Streamer Pressure and Vertical Particle Velocity – Theory and Application to Data. *74<sup>th</sup> EAGE Conference & Exhibition*, Extended Abstracts.
- Sacchi, M.D. [1997] Reweighting Strategies in Seismic Deconvolution. *Geophysics Journal International*, **129**, 651-656.
- Trad, D., Ulrych, T. and Sacchi, M. [2003] Latest Views of the Sparse Radon Transform. *Geophysics*, **68**, 386-399.
- Wang, P. and Peng, C. [2012] Premigration Deghosting for Marine Towed Streamer Data. *82<sup>nd</sup> SEG Annual International Meeting*, Expanded Abstracts, 1-5.
- Wiggins, R.A. [1978] Minimum Entropy Deconvolution. *Geoprospection*, **16**, 21-35.
- Yang, F., Sablon, R., and Soubaras, R. [2015] Time Variant Amplitude and Phase Dispersion Correction for Broadband Data. *85<sup>th</sup> SEG Annual International Meeting*, Expanded Abstracts, 4620-4625.